

Perylene-Derivative Langmuir–Blodgett Films for Use as Ultrathin Charge-Transport Barriers

Marko Burghard,* Claudius M. Fischer, Michael Schmelzer, Siegmund Roth, Michael Hanack,[†] and Wolfgang Göpel[‡]

Max-Planck-Institut für Festkörperforschung, Heisenbergstr. 1, D-70569 Stuttgart, Germany

Received April 25, 1995. Revised Manuscript Received August 29, 1995[§]

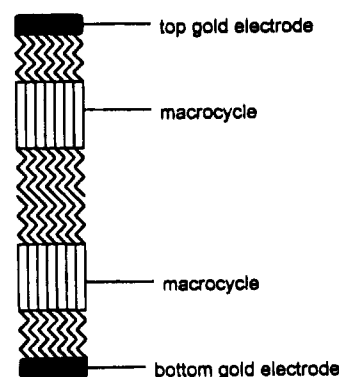
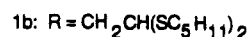
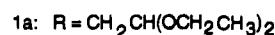
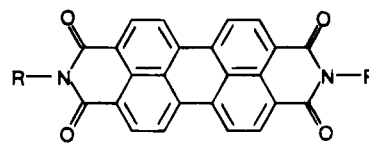
Very thin sandwich structures composed of two different perylene-3,4,9,10-tetracarboxyldiimide derivative Langmuir–Blodgett (LB) films, symmetrically contacted with microstructured gold electrodes, have been prepared. The nature of the side chains on the π -system influences the Langmuir layer behavior and the presence of sulfur appears to increase the ability to withstand the evaporation of the top gold electrode. At 4 K, both junctions exhibit abrupt current onsets at reproducible voltage thresholds that make these LB layers useful as well-defined tunneling barriers with respect to molecules with lower ionization potential. There is evidence for tunneling processes involving the highest occupied molecular states at low temperatures, whereas increasing temperature leads to the dominance of hopping conductivity.

Introduction

There is still growing interest in building electronic devices from highly ordered organic films. The Langmuir–Blodgett (LB) technique has often been used to prepare thin organic assemblies, but the problem of contacting these films slowed down progress toward real devices. In fact, the preparation of sandwich structures that incorporate ultrathin LB films has been impeded by a number of serious practical problems leading to short circuits.¹ As a consequence, bottom electrode metals with natural oxide layers were mostly used.² The electrical behavior of such structures is always determined by both the organic material and the inorganic layer. Only more recently, Iwamoto et al. reported on inelastic tunneling spectroscopy performed with junctions of polymer LB films using gold as bottom electrode.³

To directly observe the electrical properties of organic systems, it is advantageous to use a noble metal for both the bottom and top contact. Recently, we reported on the electrical-transport properties of an ultrathin LB heterostructure⁴ consisting of a peripherally octapentyloxy-substituted palladium phthalocyanine and a perylene-3,4,9,10-tetracarboxyldiimide derivative (**1a**) sandwiched between two gold electrodes (Scheme 1). Noteworthy, the expected film structure is such that the π -systems are separated from each other and from the electrodes by relatively short insulating aliphatic chains. The current/voltage curves at 4.2 K showed rectifying behavior and, in addition, current steps for the situation

Scheme 1. Chemical Structure (Top) of Perylene-3,4,9,10-tetracarboxyldiimide Derivatives 1a and 1b and Schematic Side View (Bottom) of a Sandwich Device



that the electrode close to the perylene derivative was positively biased. We ascribed these steps to Coulomb-blockade charging effects because they occurred at voltages in good agreement with theoretical assumptions. Further, we attributed the ability of the perylene derivative film to function as a barrier for hole injection into the phthalocyanine units to the HOMO levels of these molecules lying energetically deeper than the HOMO levels of the phthalocyanine. However, at the present stage, the role of defects, both inherent to the structure or introduced by the evaporation of gold, is still open. For future studies, molecular building blocks are needed which allow a proper adjustment of the LB

[†] Universität Tübingen, Lehrstuhl für organische Chemie II, Auf der Morgenstelle 18, D-72076 Tübingen, Germany.

[‡] Universität Tübingen, Institut für physikalische Chemie, Auf der Morgenstelle 18, D-72076 Tübingen, Germany.

[§] Abstract published in *Advance ACS Abstracts*, October 1, 1995.
(1) Couch, N. R.; Montgomery, C. M.; Jones, R. *Thin Solids Films* **1986**, *135*, 173.

(2) Roberts, G. *Langmuir-Blodgett Films*; Plenum: New York, 1990; Chapter 4.

(3) Iwamoto, M.; Wada, M.; Kubota, T. *Thin Solid Films* **1994**, *243*, 472.

(4) Fischer, C. M.; Burghard, M.; Roth, S.; v. Klitzing, K. *Europhys. Lett.* **1994**, *28*, 129.

film thicknesses and the HOMO positions in the two layer materials. Compound **1b** has been designed such that the four sulfur atoms should lead to binding interactions with gold atoms of the top electrode, thus reducing the possibility of metallic filament formation so that thinner films can be contacted. The affinity of sulfur toward gold surfaces can be used for the self-assembly of monolayers.⁵ In the present case, things are changed such that gold atoms from the vapor phase should be attracted by sulfur centers on the surface of the LB film. Interactions between evaporated metal atoms and functionalized organic surfaces have been demonstrated for, e.g., the interface between copper and carboxylic acid-terminated self-assembled monolayers.⁶

Experimental Methods

The perylene-3,4,9,10-tetracarboxyldiimide derivative **1a** was synthesized by condensation of perylene-3,4,9,10-tetracarboxyldianhydride with 2-aminoacetaldehyde diethyl acetal in molten imidazole in a procedure similar to that described by Rademacher et al.⁷ The product was isolated by Soxhlet extraction with chloroform and further purified by repeated crystallization from chloroform. **1b** was obtained by transesterification of **1a** with excess *n*-pentanethiol and a catalytic amount of *p*-toluenesulfonic acid in chloroform. Purification was achieved by column chromatography (SiO₂; CH₂Cl₂ as eluent). The structure of both compounds was confirmed by NMR spectroscopy and elemental analysis. A 0.5 mM chloroform solution of **1a** (in the case of **1b**: 2mM) was spread onto a LAUDA trough equipped with a film lift FL-1. All operations were conducted under clean room conditions (particle class 1000). Vertical transfer of **1b** was performed with a dipping speed of 4 mm/min in both directions. The substrate was oriented in such a way that the bottom electrode stripes were perpendicular to the dipping direction. In the case of horizontal transfer of **1a**, the substrate was removed from the water surface with a speed of 2 mm/min. Small-angle X-ray diffraction was performed with a Siemens D500 diffractometer in Bragg-Brentano geometry (Cu K α line, $\lambda = 1.54 \text{ \AA}$). The Si(111) wafer were treated with diluted hydrofluoric acid to remove the oxide layer. For UV/vis spectroscopy, films were transferred onto Suprasil glass slides that have been rendered hydrophobic by treatment with a solution of hexamethyldisilazane in chloroform. Optical absorption spectra were recorded with a Perkin Elmer Lambda 2 spectrometer. As bottom electrodes we used 95 \AA thick gold films prepared by a photolithographical process on highly polished BK7 glass substrates ($7 \times 7 \text{ mm}^2$). The top gold electrodes were evaporated to a thickness of 150 \AA in stripes perpendicular to the bottom electrodes, forming junctions with an active area of $30 \times 100 \text{ }\mu\text{m}^2$. Lateral conductivity of these electrodes was confirmed by measuring their resistivity. Current/voltage curves were recorded with a Keithley 617 electrometer.

Results and Discussion

LB Films: Structural and Optical Properties.

The area per molecule on a pure water subphase was determined from the surface pressure/area isotherms to be 54 \AA^2 for **1a** and 68 \AA^2 for **1b**. By modeling the molecular dimensions with computer simulation,⁸ it is found that these values are too large for the molecules standing upright on their short edge but also too small

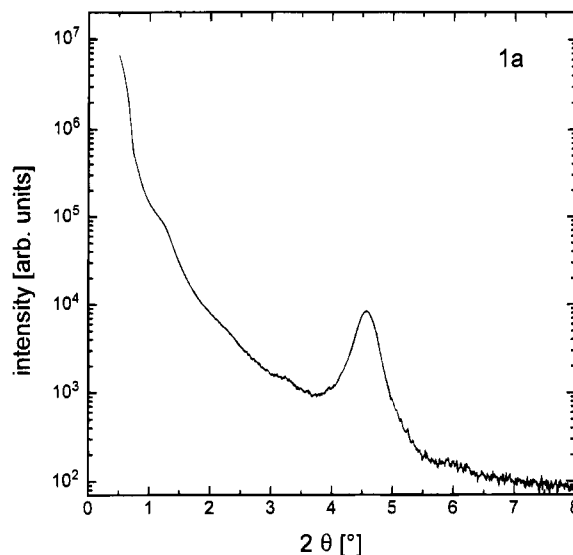


Figure 1. Small-angle X-ray diffraction curve for a 40 monolayer LB film of **1a** on Si(111).

for them lying flat on the water surface. The small-angle X-ray scattering curve for a 40 monolayer LB film of **1a** on Si(111) is depicted in Figure 1. The Bragg (001) reflection is observed at $2\theta = 4.6^\circ$, corresponding to a layer spacing of $d = 19.5 \text{ \AA}$. In comparison, the scattering curve for **1b** (not shown) exhibits well-developed Kiessig fringes and a somewhat broader peak at $2\theta = 5.5^\circ$, leading to a d value of 16 \AA . In view of these results, we propose an arrangement of the ring systems standing on their short edge but tilted against the surface normal.

Compound **1a** forms a stable monolayer at the air/water interface at 10°C and a surface pressure of $\pi = 20 \text{ mN/m}$, while the monolayer of **1b** stabilizes after a small structural reorganization at 4°C and $\pi = 12 \text{ mN/m}$. At the indicated surface pressure values, the Langmuir layers can be transferred onto, e.g., hydrophobic glass, ITO, silver, and gold substrates and also very efficiently on top of the above-mentioned octasubstituted palladiumphthalocyanine LB films.⁹ While transfer of compound **1a** is possible only by a horizontal technique,¹⁰ **1b** can be vertically transferred as a Y-type film (transfer ratios close to 1.0). The vertical transfer is more desirable because it allows a slower movement of the meniscus, what is known to result in lower defect densities.

Figure 2a displays the optical absorption spectrum of the chloroform solution of **1b** together with the absorption spectra of 6-monolayer LB films of **1a** and **1b**. The solution spectrum exhibits maxima at 434, 460, 490, and 528 nm corresponding to vibronic transitions of the perylene chromophore¹¹ and is almost identical for both compounds. This finding is expected, because the different substituents are not electronically coupled to the perylene π -system. In the films, the bands are broadened and prominent peaks are found at 472, 494, 546, and 581 nm for **1a** and at 476, 510, and 561 nm in the case of **1b**. The absorbance of the **1b** film is about twice the absorbance of the **1a** film because for the latter

(5) Schierbaum, K. D.; Weiss, T.; Thoden van Velzen, E. U.; Engbersen, J. F. J.; Reinhoudt, D. N.; Göpel, W. *Science* **1994**, *265*, 1413.

(6) Smith, E. L.; Alves, C. A.; Anderegg, J. W.; Porter, M. C.; Siperko, L. M. *Langmuir* **1992**, *8*, 2707.

(7) Rademacher, A.; Märkle, S.; Langhals, H. *Chem. Ber.* **1988**, *121*, 225.

(8) Hyperchem 4.0, Autodesk, Inc. 1994.

(9) Burghard, M.; Schmelzer, M.; Roth, S.; Haisch, P.; Hanack, M. *Langmuir* **1994**, *10*, 4265.

(10) Nakahara, H.; Fukuda, K. *J. Colloid Interface Sci.* **1979**, *69*, 24.

(11) Ferguson, J. *J. Chem. Phys.* **1966**, *44*, 2677.

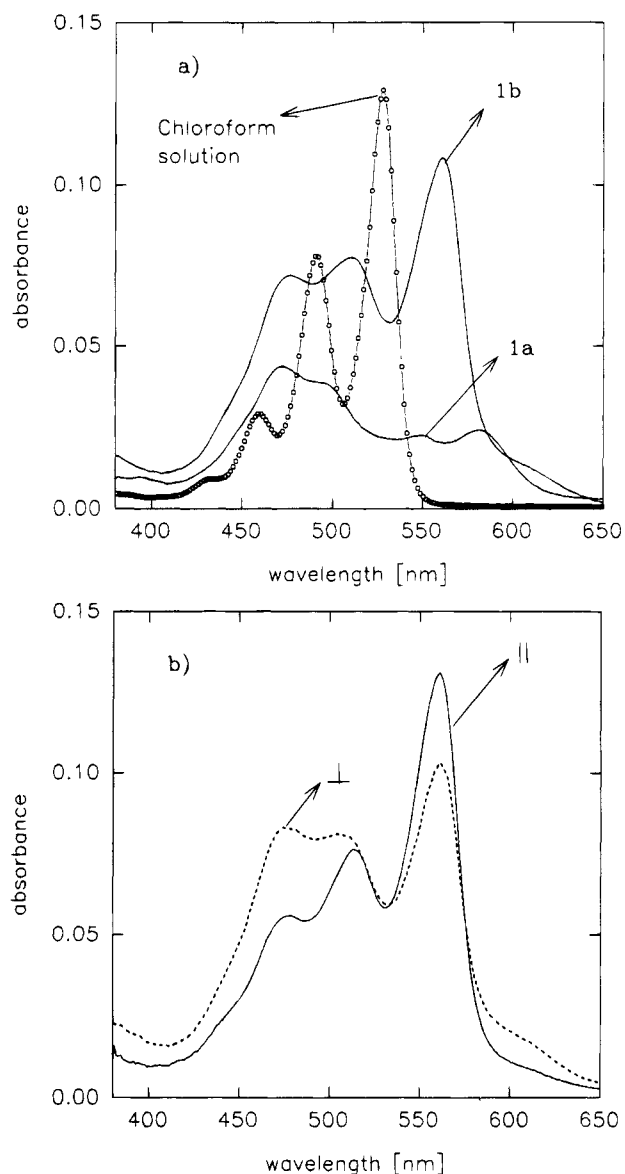


Figure 2. (a) Optical absorption spectra of **1b** in chloroform solution and 6 monolayer LB films of **1a** and **1b**, (b) polarized spectra for LB film of **1b** with electric field vector parallel (full line) and perpendicular (broken line) to dipping direction.

only one side of the substrate is covered during horizontal transfer. For both compounds the absorption spectra are almost identical for films of one and six monolayers, respectively, indicating that the electronic interactions arise between molecules in the same monolayer and not between molecules in adjacent layers. The transition dipole moment of the visible band lies in the long axis of the perylene ring plane.¹² Thus it follows that in both films the perylene rings cannot stand perfectly upright on their short edge. Interpretation of the solid-state spectra is complicated because vibrational splitting and band shifts due to excitonic interactions might simultaneously occur. We assume that in both films a red as well as a blue shift of the visible band, relative to the solution spectrum, is observed. Such a spectral band pattern can be understood in terms of exciton coupling arising from (at least) two translationally nonequivalent molecules in the unit cell,

(12) Tanizaki, Y.; Yoshinaga, T.; Hiratsuka, H. *Spectrochim. Acta* **1978**, *34A*, 205.

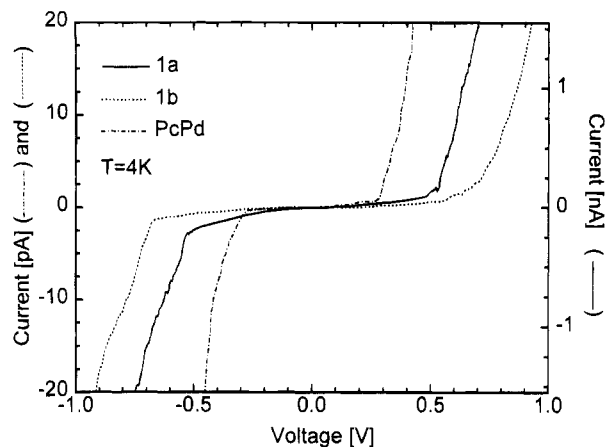


Figure 3. *I/V* curves for (gold/20 monolayer LB film/gold) devices of **1a** (full line) and **1b** (dotted line) and peripherally octa(pentyloxy)-substituted palladium phthalocyanine (PcPd, dashed line) at 4.2 K. The junction area is in each case $30 \times 100 \mu\text{m}^2$.

which is also known for, e.g., the β -modification of phthalocyanines.¹³ With linearly polarized light in normal incidence, the LB film of **1a** does not show any dependence on the polarization direction, while the film of **1b** yields different spectra (Figure 2b) for polarization parallel and perpendicular to the dipping direction. In the latter case, the long-wavelength band is more intense when the electric field vector is polarized parallel to the dipping direction. A similar observation has been documented for LB films of, e.g., amphiphilic phthalocyanines.¹⁴ The presence of more flexible pentythio groups in **1b** seems to provide a higher fluidity to the film so that flow orientation of the molecular columns, likely during film deposition, becomes possible.

LB Films: Electrical Properties. Sandwich structures were prepared from both films using gold electrodes as both bottom and top contact. Compound **1b** proved to be especially stable against application of a gold top electrode. For a given number of monolayers, the yield of nonshorted junctions was improved by a factor of about 2 for films of **1b** as compared to **1a**. In addition, we were able to obtain nonshorted devices incorporating heterostructures that consist of only 4 monolayers **1b** on top of 4 monolayers of an octa(pentyloxy)-substituted metallophthalocyanine LB film, which was impossible with compound **1a**. The current (*I*)/voltage (*V*) curves at 4.2 K for sandwich structures consisting of 20 monolayers of **1a** and **1b**, respectively, are depicted in Figure 3 (the junction area in both cases is $100 \times 30 \mu\text{m}^2$). These *I/V* characteristics could be observed for different contacts on the same substrate. They display symmetric behavior, which points to a similar electronic behavior at the two metal/organic film interfaces. Hence it can be concluded that there is no critical destruction of the film molecules at the top electrode contact as this would result in different defect densities at the top and bottom interface. Note that the current is remarkably lower for compound **1b** compared to **1a**. One possible explanation for this observation is the presence of longer aliphatic chains in **1b** which separate the π -systems in adjacent layers, thereby

(13) Lyons, L. E.; Walsh, J. R.; White, J. H. *J. Chem. Soc.* **1960**, 167.

(14) Poynter, R. H.; Cook, M. J.; Chesters, M. A.; Slater, D. A.; McMurdo, J.; Welford, K. *Thin Solid Films* **1994**, *243*, 346.

increasing the sum of interlayer tunnel distances. The lower current might also be connected with a larger effective thickness (expressed in the number of electrically active monolayers) of the **1b** junction.

Abrupt current increases occur at ± 0.55 V for the film of **1a** and at ± 0.68 V for **1b** reproducibly for different contacts. The same voltage thresholds are observed upon repeated scans, and also for different film thicknesses (6, 10, and 20 monolayers), roughly the same values are obtained. Figure 3 also shows the I/V characteristic of a 20 monolayer sandwich structure incorporating the above-cited palladiumphthalocyanine. For this material, current onsets are observed already at ± 0.27 V. The voltage shift of more than 0.1 V upon going from **1a** to **1b** represents a useful expansion of the barrier behavior with respect to the current onset of the phthalocyanine compound, the ionization potential of which is lower than for the perylene derivatives. This shift might be due to the longer aliphatic chains in **1b** separating the π -systems and/or to the different packing of the π -systems in both films, which would alter the ability to delocalize charge between neighboring rings in the film plane (in this way reflecting the different relative orientations of adjacent chromophores in both types of films as revealed by the optical absorption spectra).

At liquid helium temperature, thermionic processes should be frozen out while tunneling processes should dominate. Electron injection through tunneling from the gold into the conduction band is less expected because of the considerable offset between the gold Fermi level and the estimated LUMO position¹⁵ of the perylene derivative. Thus, the barrier (neglecting the presence of the insulating aliphatic chains) for carrier injection is more likely the difference between the gold's Fermi energy (5.1 eV¹⁶) and the HOMO level of the molecules. Further, we attribute the sharpness of the current onsets to a resonance-like energetic match between the perylene derivative HOMO level and the gold Fermi edge leading to hole injection into the organic material. This model should hold for both bias directions. The applicability of a simple barrier model might be tested in order to obtain first information about the charge-transport mechanism. The tunneling current I at voltage V through a triangular barrier of thickness d and height Φ is described by eq 1 according to the Fowler-Nordheim model,¹⁷ where m^* is the effective mass of the carriers with charge q .

$$\frac{I}{V^2} \propto \exp\left[\frac{-8\pi\sqrt{2m^*}(q\Phi)^{3/2}d}{3hqV}\right] \quad (1)$$

The logarithmic plots of (I/V^2) versus V^{-1} for the 20 monolayer devices of **1a** and **1b** are given in Figure 4. The data fit well to the straight line in the higher field region. Assuming that the above mentioned voltage thresholds represent the corresponding barrier heights, the barrier thickness is calculated from the straight line fit in the case of **1a** to 4.5 Å (m^* is taken as the free electron mass). For **1b** we obtained a value of 5 Å. In

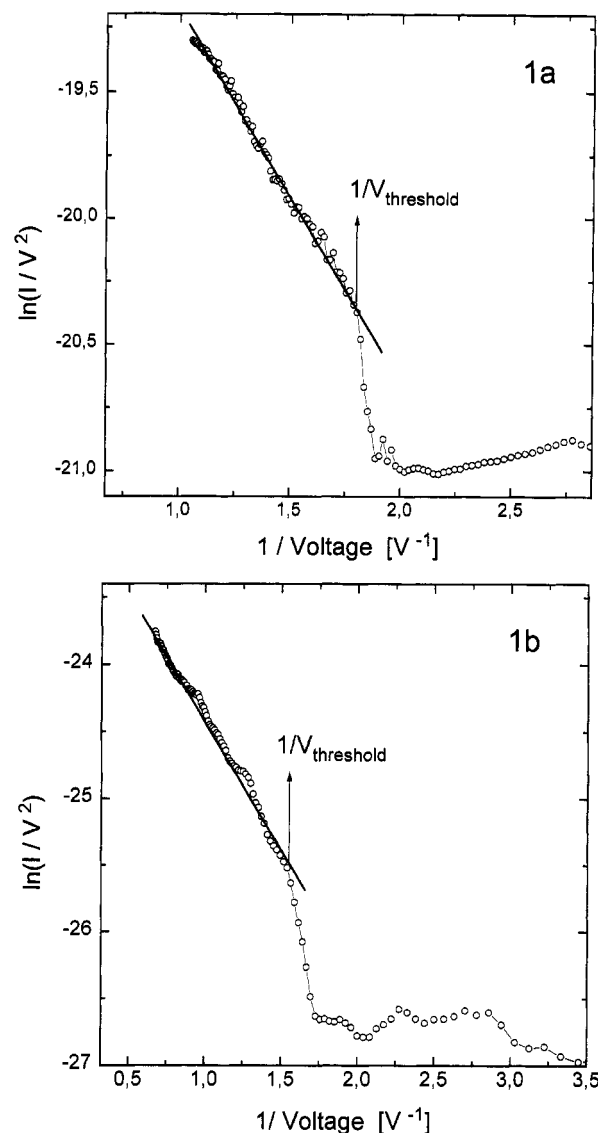


Figure 4. Fowler-Nordheim plot for the 20 monolayer device of **1a** (top) and **1b** (bottom) at 4.2 K.

both cases, the beginning of the straight-line fit corresponds to the voltage threshold. These thresholds are indeed close to the estimated offset (≈ 0.5 – 0.8 eV) between the HOMO position¹⁸ of the perylene-tetracarboxyldiimide derivatives and the work function of gold. However, using the small-angle X-ray diffraction results, the film thicknesses are calculated to 400 Å for **1a** and 320 Å for **1b**, which are considerably larger than the barrier thicknesses obtained from the Fowler-Nordheim plot. Even though at the present stage we cannot exclude the formation of metallic filaments reaching into the film, the value of 4.5 Å (respectively 5 Å) is too small to represent the effective film thickness. There appear two possible explanations for this discrepancy.

First, the additional tunneling barriers constituted by the aliphatic chains between the adjacent layers could have a profound influence on the interlayer tunneling events and should therefore not be neglected. In this case, the tunneling probability would have to be calculated by integrating the different damping constants of the electron wave function (corresponding to the σ - and

(15) Danziger, J.; Dodelet, J.-P.; Lee, P.; Nebesny, K. W.; Armstrong, N. R. *Chem. Mater.* **1991**, *3*, 821.

(16) Michaelson, H. B. *J. Appl. Phys.* **1977**, *48*, 4729.

(17) Fowler, R. H.; Nordheim, L. W. *Proc. R. Soc. London Ser. A* **1928**, *119*, 173.

(18) Karl, N.; Sato, N. *Mol. Cryst. Liq. Cryst.* **1992**, *218*, 79.

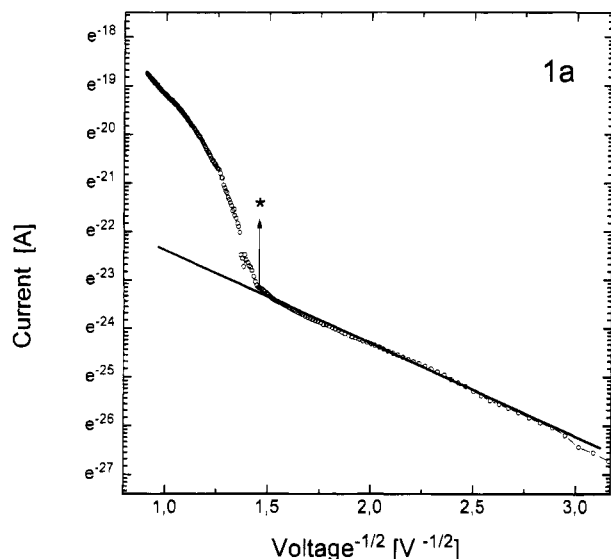


Figure 5. Logarithmic plot of current versus $1/\sqrt{V}$ for the 20 monolayer junction of **1a** at 4.2 K; the star corresponds to 0.5 V.

π -bonded regions according to Scheme 1) over the distance from the electrode surface. Consequently, the assumption of a triangular barrier does not longer hold and eq 1 is an inadequate description.

A second possibility is that already at low voltages, there is an excess current due to tunneling through localized gap states (which continues also above the voltage threshold, although its contribution to the total tunneling current might be low). A similar model of sequential tunneling via a chain of localized states has recently been proposed by Raikh et al.¹⁹ for a conjugated polymer device and they predicted a current/voltage relationship of $\ln I \propto 1/\sqrt{V}$. The logarithmic plot of current I versus $1/\sqrt{V}$ for the 20 monolayer device of **1a** is shown in Figure 5. The linear fit to the plot seems reasonable up to 0.5 V (marked with a star). Also, the contribution of an additional tunneling current below the voltage threshold is apparent. At a value slightly above 0.5 V, the onset in the corresponding Fowler–Nordheim plot is observed (Figure 4, $1/V_{\text{threshold}} \approx 1.9V^{-1}$). The voltage of about 0.5 V might therefore be considered as the transition point from which on direct tunneling of holes from the electrodes into the HOMO states dominates over the sequential tunneling mechanism. A similar behavior is found for films of **1b** with a higher transition voltage (≈ 0.6 V). Injected charge is expected to lead to strong local distortions of the electrical field in the film. Hence, due to the charge transport via tunneling between the gap states, the field distribution between the electrodes must not necessarily be homogeneous when the transition voltage for direct tunneling is reached. The small slopes of the Fowler–Nordheim plots in Figure 4 could therefore be explained by a relatively small effective barrier thickness, i.e., the voltage drops mainly close to one electrode/organic film interface and the barrier height could be close to the value of the voltage threshold for the current onsets. Direct tunneling of holes into the occupied molecular states then involves only the first or two first monolayers close to the electrode. There still remains, of course,

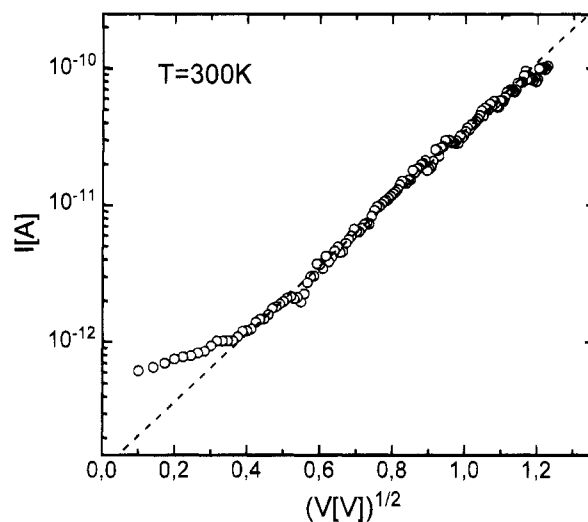


Figure 6. Logarithmic plot of current versus $V^{1/2}$ for the 20 monolayer device of **1b** at room temperature.

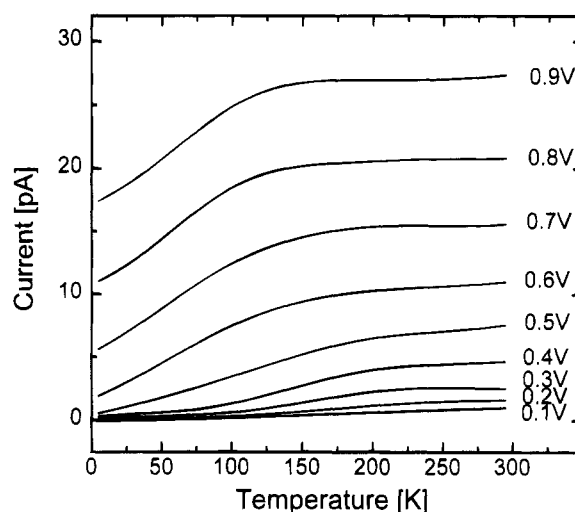


Figure 7. Temperature dependence of current at different voltages for 20 monolayer device of **1b**.

the requirement that the remaining barrier is approximately of triangular shape.

With increasing temperature, the sharp current onsets are getting washed out and a $\log I \propto V^{1/2}$ behavior is observed, as shown in Figure 6 for **1b** as representative example at room temperature. Such a current/voltage relationship has also been observed for other LB film systems²⁰ and has been interpreted in terms of field-assisted charge carrier detrapping (Poole–Frenkel effect) or thermionic carrier injection from the electrodes (Schottky emission). These charge-transport mechanisms require an exponential dependence of current on temperature. The change of current with temperature is demonstrated in Figure 7 for different voltages. The important result is that, if the current is scaled to the voltage values, all curves display the same principal feature, i.e., the conductivity rises for temperatures up to about 150 K until it becomes saturated. This phenomenon is clearly not associated with an activation process over the “bandgap” but would be best explained by hopping conductivity between statistically distributed defect and/or impurity sites. In light of this result,

(19) Raikh, M.; Xing, W. *Mol. Cryst. Liq. Cryst.* **1994**, *256*, 563.

(20) Geddes, N. J.; Sambles, J. R.; Parker, W. G.; Couch, N. R.; Jarvis, D. J. *J. Phys. D: Appl. Phys.* **1990**, *23*, 95.

Schottky emission or the Poole-Frenkel effect are not regarded to explain the charge-transport behavior. Instead, the weak temperature dependence indeed points to a defect-assisted hopping conductivity, which follows an $\exp(V/V_0)^\alpha$ law ($0 < \alpha < 1$) and that has been observed for a number of different polymeric or other organic semiconductors.²¹ As there is no principal difference between the curves of Figure 7 in whether the voltage is above or below the voltage thresholds, we deduce that the hopping processes occur competitively to the tunneling processes involving the HOMO levels and gain more importance the higher the temperature. Even at liquid helium temperature, tunneling between these defect sites influences the "background" current between the voltage thresholds. It is, because we are mainly interested in the tunneling events, a future task to reduce this current as far as possible through a higher purity of the film molecules as well as an improved structural order of the films. This could also lead to the observation of the sharp voltage thresholds already at higher temperatures. That is why LB film forming

molecules are sought which can be purified by vacuum sublimation.

In conclusion, the LB films of the perylene-tetracarboxyldiimide derivatives **1a** and **1b** exhibit good stability against gold evaporation. Especially the LB film of compound **1b** is expected to be useful as an ultrathin tunneling barrier at low temperatures where hopping conduction is frozen out. Such a barrier would exhibit a well-defined "opening" which corresponds to the onset of the resonant-like tunneling involving its HOMO level. Thus, it seems attractive to study the charge transport of a junction in which two ultrathin barriers of **1b** bracket a material of lower ionization potential. Further, the presented results might also be of interest with regard to related charge-transport problems in electroluminescent devices.

Acknowledgment. This work was supported by Sonderforschungsbereich 329 Molekulare Elektronik and the ESPRIT network NEOME. We acknowledge the help of P. Loeffler and Prof. N. Karl, University of Stuttgart, with small-angle X-ray diffraction.

(21) Movaghar, B.; Yelon, A.; Meunier, M. *Chem. Phys.* **1990**, *146*, 389.

CM950185M